ARTICLE

Check for updates

Transport and deposition of ocean-sourced microplastic particles by a North Atlantic hurricane

Anna C. Ryan [1✉], Deonie Allen[2], Steve Allen[1], Vittorio Maselli [1✉], Amber LeBlanc [3], Liam Kelleher[4], Stefan Krause [4,5], Tony R. Walker [3] & Mark Cohen [6]

The atmosphere can transport large quantities of microplastics and disperse them throughout the globe to locations inaccessible by many other transport mechanisms. Meteorological events have been proven to pick up and transport particulate matter, however, how they influence the transport and deposition of atmospheric microplastics is still poorly understood. Here we present samples of atmospheric fallout collected during Hurricane Larry as it passed over Newfoundland, Canada in September 2021. During the storm peak, 1.13×10^5 particles m^{-2} day^{-1} were deposited, with a decline in deposition after the storm passed. Back-trajectory modelling and polymer type analysis indicate that those microplastics may have been ocean-sourced as the hurricane traversed the garbage patch of the North Atlantic Gyre. This study identifies the influence of North Atlantic hurricanes on the atmospheric transport and deposition of ocean-sourced microplastics and the possible consequences of increased exposure to microplastics in remote areas.

[1] Department of Earth and Environmental Sciences, Dalhousie University, Halifax, NS, Canada. [2] Department of Civil and Environmental Engineering, University of Strathclyde, Glasgow, UK. [3] School for Resource and Environmental Studies, Dalhousie University, Halifax, NS, Canada. [4] School of Geography, Earth and Environmental Sciences, University of Birmingham, Birmingham, UK. [5] Ecologie des Hydrosystèmes Naturels et Anthropisés (LEHNA), Université Claude Bernard Lyon, Lyon, France. [6] Air Resources Laboratory, National Oceanic and Atmospheric Administration, College Park, MD, USA. ✉email: anna.c.ryan@dal.ca; vittorio.maselli@dal.ca

Microplastic (MP) pollution is a growing environmental and public health concern that has been detected in all environments around the globe[1–4] with the risk of causing significant harm to humans, wildlife, and overall ecosystem health, as well as affecting climate processes[5–10]. MPs are generally sourced in continental regions with high levels of anthropogenic activity and then are transported, primarily by rivers, to oceans[11–13]. Therefore, most MP research during the last decade has focused on describing the abundance, composition, suspected sources, and impacts of MPs in such environments[14–19]. Thus, the fate and transport processes of MPs in the atmosphere were not as thoroughly investigated.

Recent studies, however, have determined that the atmosphere may play a crucial role in the transport and deposition of MPs, especially in remote terrestrial regions that have no local source of plastic pollution[1,4,20]. Furthermore, it has been shown that the ocean, so far considered a long-term sink for MPs, can also act as a source of plastic pollution, with small MPs escaping from the sea surface into the atmosphere via bubble burst ejection or wave action, allowing for a potentially continuous cycle of transport and deposition of MPs[21]. The idea that MPs could be transported through the air as well as by ocean waters has opened a new paradigm in plastic research, questioning for instance how major weather events such as tropical or extratropical storms may affect MP transport pathways, deposition patterns, and amounts. Previous studies have found that intense precipitation can increase the abundance of larger atmospheric MP fallout, while high winds and storm systems can broaden the potential transport distances[22,23]. These observations suggest hurricanes, known for intense precipitation and sustained high winds, could be able to transport MPs across oceans faster than oceanic currents and increase deposition amounts to places that may not receive regular MP deposition from other sources.

Hurricanes in the North Atlantic Ocean usually form off the west coast of Africa, gaining energy as they travel across warm tropical waters and then dissipate over land or colder waters along the east coast of North America. Hurricanes can span hundreds of kilometres in diameter and have winds exceeding 250 km h^{-1} [24]. Such strong winds at ground level have the capability to resuspend large amounts of terrestrial particulate matter, including pollutants, into the atmosphere and transport them, along with particulate matter already in the air, for thousands of kilometres[25,26]. Increased wave activity and strong winds at the sea surface can also resuspend particles entrained in ocean surface waters[21,27,28], whereas heavy rains associated with hurricanes wash particles and pollutants out of the atmosphere, depositing them in locations that could be at a far distance from their source[29]. This has been demonstrated, for example, by the presence of frozen plankton in ice crystals of cirrus clouds over Oklahoma after Hurricane Nora in 1997[30], or by the elevated levels of air pollutants, including particulate matter ($PM_{2.5}$), after Hurricane Florence struck North Carolina in 2018[31]. Consequently, hurricane-driven transport may represent an important mechanism for dispersing MPs to remote locations.

In this study, we investigated the impact of Hurricane Larry on atmospheric MP deposition in the North Atlantic region by collecting air samples from before, during, and after the passage of the hurricane over Newfoundland, Canada, where it made landfall as a Category 1 hurricane on 11 September 2021[32] (Fig. 1). The island of Newfoundland has very low population density (1.4 person km^{-2})[33], with most of the population living in the provincial capital, St. John's, leaving the rural areas sparsely inhabited. Due to the limited presence of industries beyond the capital city[34], most rural areas, particularly in the island's interior, do not possess significant sources of atmospheric MPs. This implies that, apart from coastal and river floodplain regions, the predominant mode for transporting MPs to these remote areas is through the atmosphere. Newfoundland frequently experiences various weather events such as extratropical cyclones, nor'easters, and hurricanes[35,36]. These weather phenomena can exert a considerable influence on the deposition of atmospheric MPs, making Newfoundland an analogue for any remote or sparsely populated mid-latitude terrestrial area that faces extreme atmospheric events. Furthermore, Hurricane Larry followed a track far offshore of the eastern seaboard of the United States and Eastern Canada, maintaining its trajectory over the ocean and traversing the North Atlantic garbage patch before making landfall in Newfoundland[37] (Fig. 1 and Supplementary Fig. 1). Thus, Hurricane Larry presented a unique opportunity to study MP deposition from a hurricane that had not travelled close to any major urban areas in a sparsely populated location with no obvious local point sources of MPs.

Results and discussion

Hurricane Larry. Hurricane Larry originated offshore the west coast of Africa (11°N, 20°W) on August 30, 2021, as a tropical depression and evolved into a category 3 hurricane on September 4 approximately 1600 km east of the British Leeward Islands before making landfall as a category 1 hurricane at 00:30 September 11 near Great Bona Cove (Newfoundland, Canada, Fig. 1)[32], approximately 130 km west of the sampling location of this study (47°11'0.15" N, 52°50'33.50" W; Fig. 1). Sample collection commenced the evening of September 9, and ended September 12, 2021, with a new sample being collected every 6 h for a total of 11 composite samples each collected over a 6-h period. The sample location experienced fair-weather conditions prior to the evening of September 10 (samples 1–3), with wind blowing mainly from the south at average speeds <22 km h^{-1}, and gradually increasing leading up to the hurricane (measured at the Cape Race weather station located approximately 60 km south of the sample site; Fig. 2). The duration of true hurricane anticyclonic activity extended from the early evening of September 10 to the morning of September 11 (samples 4, 5, and 6), with a minimum atmospheric pressure of 980 hPa and a maximum sustained wind speed of 109 km h^{-1} detected at 00:30 on September 11 (during sample 6) at the Cape Race weather station, marking the passing of the eye of the hurricane. Heavy rainfall occurred from 22:00 September 10 to 01:00 September 11, for a recorded total of 9.4 mm at Cape Race (Fig. 2). Wind direction at Cape Race shifted from the southwest during the height of the storm to gentler westerly winds after the hurricane passed (samples 7–11) with speeds between 20 and 50 km h^{-1}. No local measurements of wind speed, direction, or amount of precipitation were possible at the sample location due to a lack of equipment; however, weather data collected at Cape Race (Supplementary Fig. 2), located approximately 60 km SSW of the sample location, generally agrees with the observations made at the sampling site.

MP deposition. MPs were consistently detected in all samples, including those taken before (samples 1–3), during (samples 4–6), and after (samples 7–11) Hurricane Larry's passage over our sampling location. Notably, samples collected during the passage of the hurricane (samples 4 and 6) exhibited the highest concentration of MP particles, as illustrated in Fig. 2. Sample 6, collected shortly after recording the peak wind velocity, reached a maximum MP count of 113,569 ± 29,215 MPs m^{-2} d^{-1} (Fig. 2b). Subsequently, in sample 7, which was collected after the hurricane had passed, there was a marked decline in MP particle counts. During the hurricane, we observed the highest values for total particle counts and numbers of MPs deposited. In addition, while
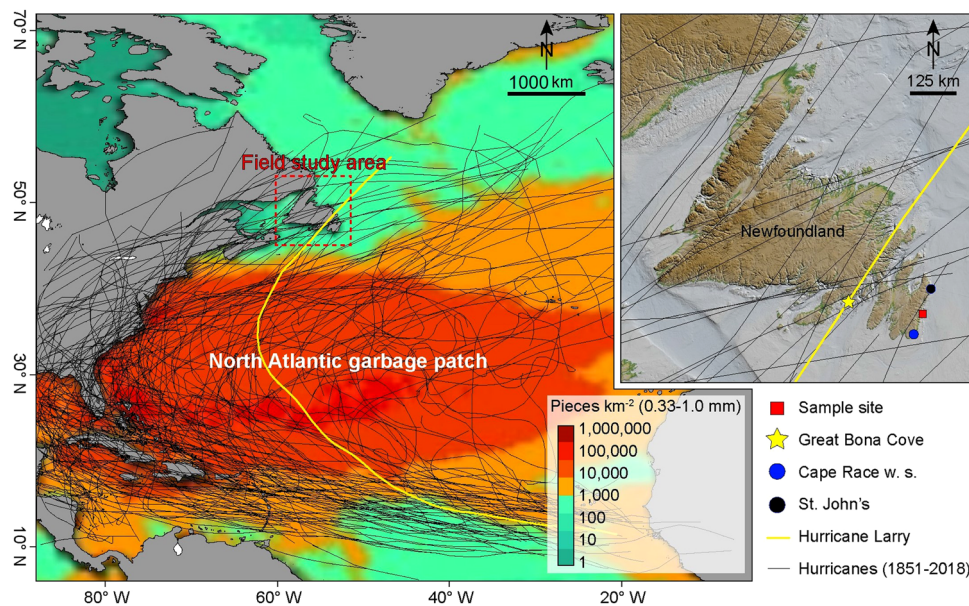
Fig. 1 Study area. Past hurricane (>category 1) tracks from 1851 to present (black lines) with Hurricane Larry track (yellow line) and plastic debris concentration (in pieces per square kilometre) in the surface waters of the North Atlantic Ocean, a possible source of microplastics found in our samples[75]. The field study area (dotted red square) is shown (inset) with the locations of the sample site (red square), Cape Race weather station where meteorological conditions were recorded (blue circle), St. John's (nearest urban area, indicated by the black circle), and Great Bona Cove (location of hurricane landfall, yellow star).

the amount of MP deposited was relatively similar for pre- and post-hurricane samples (excluding sample 1), the total particle count was on average slightly higher after the hurricane in comparison to before it (Fig. 2). We also found a significant positive correlation between the total particle deposition per day and the average amount of MPs in the samples ($r = 0.97$, $p < 0.05$).

Similar to wind speed, there is an observed upward trend in particle deposition before the hurricane, followed by a decrease immediately after the hurricane, with relatively stable deposition levels afterward. A positive correlation exists between both total particle deposition and MP deposition and the maximum wind speed recorded during the sampling period ($r = 0.61$, 0.68, $p = 0.04$, 0.02, respectively). However, it's important to note that there is no significant correlation between deposition and minimum wind speed or dominant wind direction during the sample period. Additionally, there is a positive correlation between both total particle deposition and MP deposition and the total amount of rainfall ($r = 0.68$, 0.73, $p = 0.02$, 0.01, respectively). The percentage of particles identified as MP from the total amount of particles deposited remained relatively constant throughout the entire sampling period (Fig. 2c), staying within the range of 20–30%.

The deposited MPs identified in sample 1 were significantly reduced, with only 753 particles m^{-2} d^{-1} (Fig. 2). Furthermore, the percentage of MP in sample 1 was anomalously low at just 2%. Since weather conditions and the total number of particles deposited were relatively similar between sample 1 and sample 2, we decided to treat sample 1 as an anomaly that may be due to human error during collection or analysis, and thus it was excluded from all statistical analyses. The sampling vessel broke due to high winds during sample 6 introducing possible loss of sample, though both MP and total particle deposition were still much higher than other samples.

Comparison to previous deposition. Few studies currently exist on atmospheric MP deposition during a storm event. In the South China Sea, a peak deposition of 2014 MPs m^{-2} d^{-1} was obtained during the passage of Typhoon Sinlaku[23], while 22,608 MPs m^{-2} d^{-1} were detected during monsoon rains in Iran[38]. During the passage of Hurricane Larry over Newfoundland, we recorded a maximum MP count of $113{,}569 \pm 29{,}215$ MPs m^{-2} d^{-1}. This is a significantly higher value, particularly when considering that our sampling site was in a remote location whereas the other studies collected samples close to densely populated urban regions[23] or in an urban centre[38]. These results may indicate that the North Atlantic Ocean was the likely source of such a high concentration of MPs detected in our samples.

Counts of atmospheric MP deposition in remote locations during non-storm conditions typically fell within the range of ca. 500 to 6000 MPs m^{-2} d^{-1} [1,20,39]. In our investigation, the samples taken before (samples 1–3) and after (samples 7–11) Hurricane Larry's passage over the sampling site presented an MP count between 700 and 30,000 MPs m^{-2} d^{-1}. While these values are comparable, they tend to be higher, and this discrepancy may either suggest that these samples could have been influenced by the hurricane's winds, given the extensive reach of the storm, or that our study site has inherently higher background MP levels than other locations, possibly due to its proximity to the ocean.

The percentage of MPs relative to total particle deposition (between 20 and 30%) after digestion and density separation agrees with previous studies[40,41], evidencing that there is an overall increase in atmospheric deposition during storm events and thus highlights how hurricanes can input substantial amounts of MPs to locations that would otherwise most likely experience very little MP deposition. The sample site chosen for this study had no local (within a 100 km radius) sources for MP pollution as it is located in a rural area and received onshore winds, meaning the main mechanism for MP deposition to this area is likely to be atmospheric fallout. Hurricanes affect a much larger area than just where the eye hits so increased deposition would be expected on a regional scale.

So far, Newfoundland has rarely experienced hurricanes greater than Category 1, such as Hurricane Larry. However, the warming of the North Atlantic Ocean due to anthropogenic
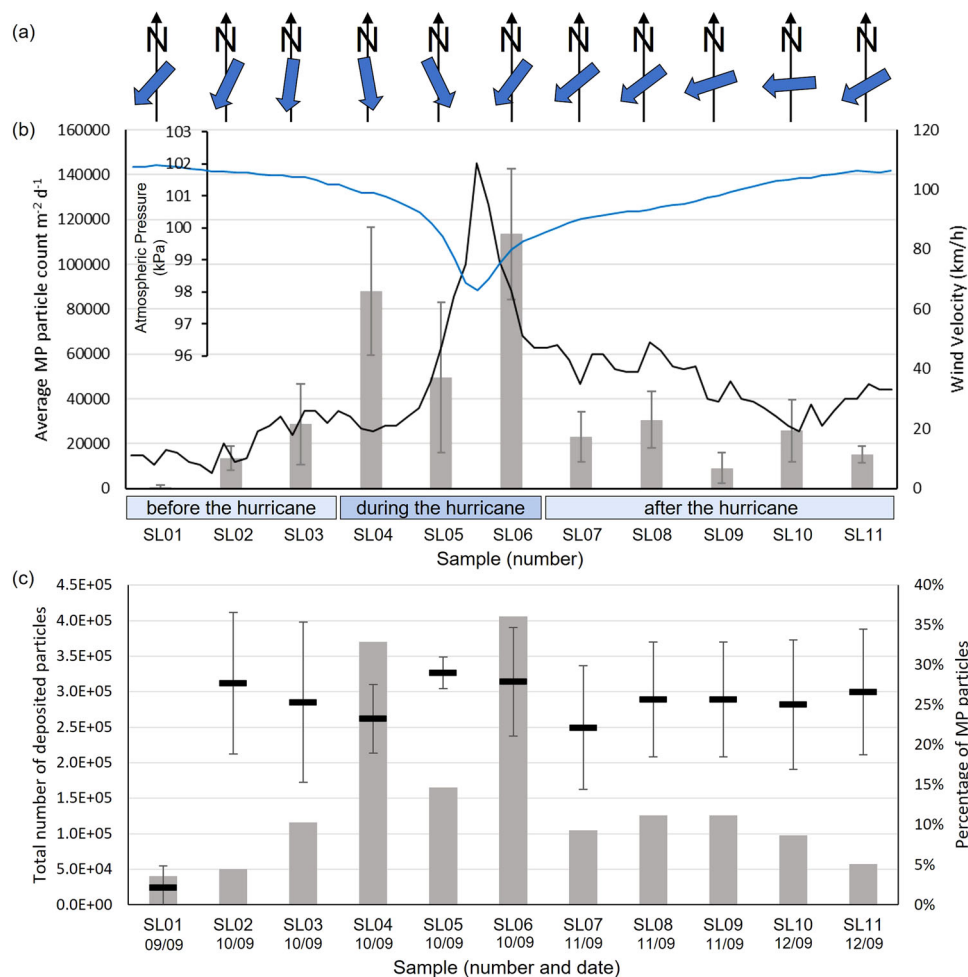
Fig. 2 MP abundance and weather conditions. a Dominant wind direction (indicated by the blue arrow) during the sample period observed at the sample site at the beginning of each sample period, **b** average microplastic (MP) particle count (with error bars representing 1σ) for each sample period (in m^{-2} d^{-1}) with wind speed indicated by a black line and atmospheric pressure indicated by the blue line (collected at Cape Race weather station) showing increase in microplastic deposition in samples collected during the hurricane, and **c** percentage of microplastic particles (indicated by black bars, with error bars representing 1σ) relative to total number of particles deposited (in m^{-2} d^{-1}) during each sample showing there was not preferential deposition of microplastics and increase in deposition of all particles during hurricane conditions, with date of sample commencement indicated below. Sample 1 may be contaminated, indicated by an anomalous proportion of microplastics to total particles.

climate change is expected not only to increase the intensity, duration, and frequency of hurricanes[42] but also to promote a northward shift in their trajectory, thus posing remote areas at higher latitudes at increasing risk of atmospheric plastic pollution. This study does not only evidence this risk for the first time but also provides a baseline to evaluate the relation between hurricane intensity and MP fallout for future events.

Particle size, shape, and polymer composition. The limit of quantification for particle size analyzed by Nile red fluorescence was 1.2 μm, set by the filter porosity. The majority (65%) of particles analyzed were of 2–10 μm size (Supplementary Fig. 4). Of the remaining particles analyzed, 34% were <2 μm, with particles between 10–20 μm making up only 1% of particles on average. Particles up to 100 μm were found in sample 6; with MPs between 20 and 100 μm accounting for 0.6% of the total particles analyzed in the sample. The largest particles found in all other samples were <40 μm (Supplementary Fig. 5). There was no significant correlation between MP sizes and wind speed or rainfall which was unexpected as previous literature has found larger particles deposited during precipitation[23]; however, there

was very little precipitation (<10 mm) over the course of the sampling period including during the peak of the hurricane (Supplementary Table 1).

Most of the particles identified were classified as fragments (Supplementary Fig. 5), with fibres accounting for less than 1% of the total particle count in all samples. This may be due to the small size of the particles, as fibres can break down into smaller pieces that are then classified as fragments[43,44]. Additionally, dust deposition samplers have been shown to create a deposition shadow wherein there is a decrease in sampler efficiency with increasing wind speed and particle size, as well as a preferential collection of finer particles[45]. The predominant particle sizes during the hurricane were in the same 2–10 μm range of those before and after the hurricane, with a skewed distribution towards smaller sizes. There was a slightly larger proportion of particles between 2 and 10 μm deposited during the hurricane compared to before and after, but not by a statistically significant (p-value = 0.56 > α = 0.05) amount.

Overall, the polymer composition of MPs showed little variation between individual samples (Fig. 3). Polymethyl methacrylate (PMMA) was the most abundant polymer in most samples ranging between 14 and 26% (Fig. 3), though made up
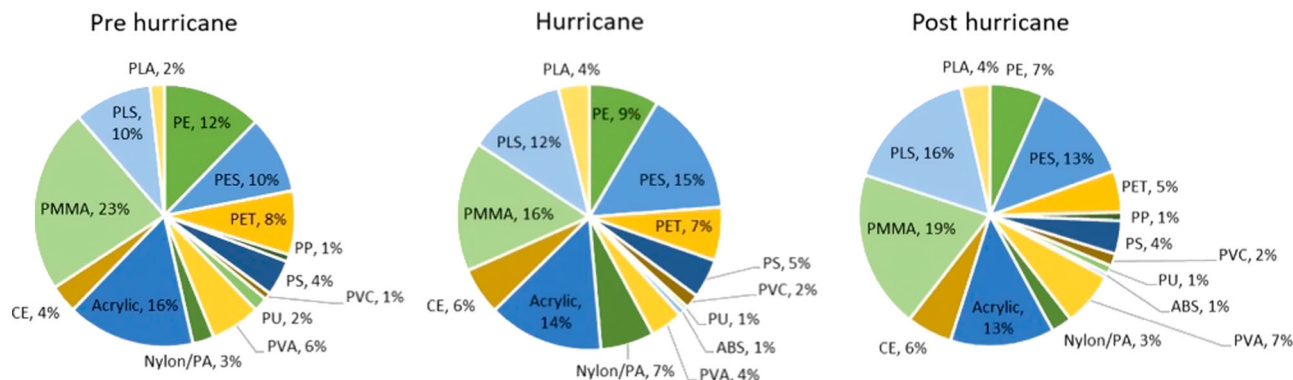
Fig. 3 Polymer types of deposited particles. The average proportion of each polymer type of microplastic particles collected before (samples 1–3), during (samples 4–6), and after (samples 7–11) Hurricane Larry (see Supplementary Table 2 for a full list of polymer names and abbreviations).

only 6% of MPs in sample 11 (Supplementary Fig. 6). This sample also had a much larger portion of polyethylene terephthalate (PET) and polyethylene vinyl acetate (PVA) than any other sample. The second most abundant polymer types were acrylic and polyester (PES), which both accounted for 14% of MPs analyzed overall. The distribution of PES MPs was relatively constant throughout the samples, except for samples 2 and 10 which only carried 3% and 7% PES particles, respectively. When comparing conditions before (samples 1–3), during (samples 4–6), and after (samples 7–11) Hurricane Larry, there is little variation in polymer proportions, although the amount of PMMA decreases during the hurricane while PES increases (Fig. 3). Acrylic is present in all samples in different amounts: MPs in sample 1 consist entirely of acrylic, which may indicate possible contamination (Supplementary Fig. 7), while acrylic particles in samples 2 represent 22% of the total, and 17% in samples 6 and 9. The proportion of nylon/polyamide (PA) was highest in samples collected during the hurricane, accounting for 7% of particles in samples 4–6 and only 3% of MPs in pre- and post-hurricane samples (Fig. 3). We found there was a positive correlation between the average MP deposition and the proportion of nylon/PA in a sample ($r = 0.71$, $p = 0.01$). There is a noticeably lower proportion of polysulfone (PLS) in samples 1 and 2 (0% and 6%, respectively), while PLS is one of the more dominant polymer types in all the other samples with the proportion of PLS MPs increasing throughout the entire sampling period.

Back-trajectory modelling. Back-trajectory modeling performed with HYSPLIT version 5.2[46,47] was used to determine possible entrainment points and pathways of air parcels that passed over the sampling site during the investigated time interval (Fig. 4). Any elevation under 1000 m above surface level is deemed to act as an entrainment point for MPs[21] as vertical mixing transports MPs lifted off the surface throughout the air column up to 1000 m[48]. Once entrained in the atmosphere, MPs in the size range investigated in this study (<100 μm) have an atmospheric lifetime of over 48 h[49], which is consistent with the length of the time window chosen for the back-trajectory analysis. The model shows that within 48 h of arriving at the sample location, a significant fraction of air parcels passed over the North Atlantic Ocean (Fig. 4), and thus possible entrainment points are from the marine environment (Fig. 5). The model also shows that some possible entrainment points are over the continent, particularly for samples 7 to 9 (Fig. 5). Nonetheless, the absence of a significant difference in polymer type and size distribution in samples 7 to 9 in comparison to the other samples with potential entrainment points over the ocean strongly indicates that the ocean remains the predominant source of microplastics in these
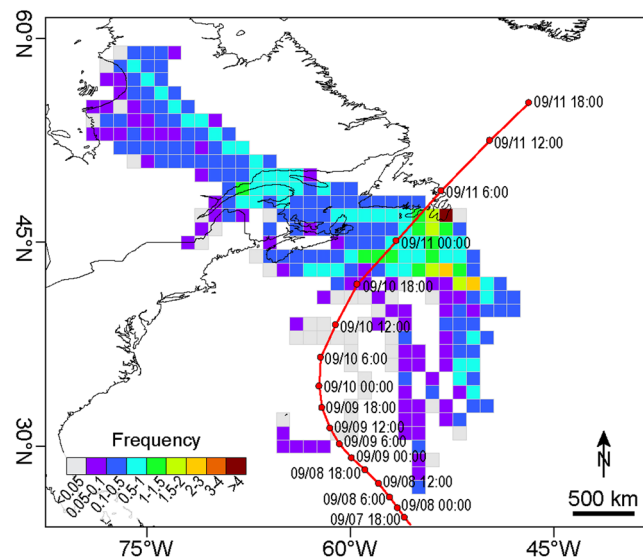

Fig. 4 Back-trajectory atmospheric modelling. Gridded frequency distribution of hourly endpoints calculated for all 48-h HYSPLIT back-trajectories ($n = 66$), started each hour within the 66-h sampling period. All endpoints from 0 to 10,000 m above ground level were included. The frequency represents the number of endpoints in each grid square divided by the total number of endpoints ($66 \times 48 = 3168$) for each 1×1-degree grid square. Hurricane Larry's track is indicated in red with the corresponding date and time.

particular samples. Sample 1 was not included in the analysis since it was considered contaminated.

Before and during the hurricane, most of the potential entrainment points were to the southwest and southeast of both the hurricane track and the sampling location, over the North Atlantic Ocean (Fig. 5), as indicated by the dominant wind directions during these periods (Fig. 2). After the hurricane passed, the potential entrainment points shifted to the west of the sample location, following the dominant wind directions (Fig. 2). Within 48 h of reaching the sample site, the air parcels generally have an elevation of <1000 m (Supplementary Fig. 8). Air parcels arriving after the hurricane, however, are generally at higher elevations, reaching over 2000 m (Supplementary Fig. 8). These air parcels also travelled for longer distances (>1000 km) in 48 h, crossing the provinces of Quebec and New Brunswick (Fig. 5). Air parcels leading up to the hurricane had the shortest transport distance between possible entrainment points and the sample site (20–35 km, see Supplementary Table 1) and were generally at lower elevations (Supplementary Table 1). Potential entrainment
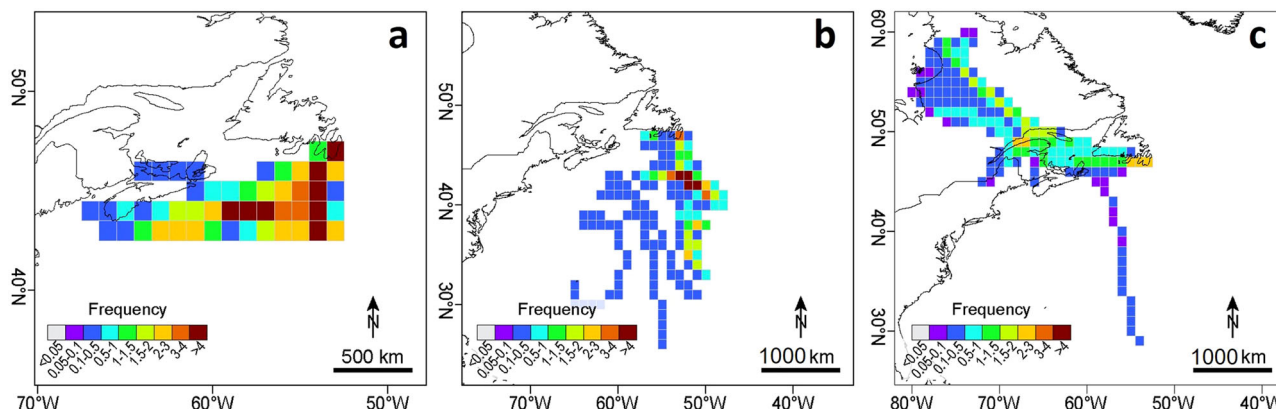
Fig. 5 Possible microplastic entrainment points. HYSPLIT air parcel 48-h back-trajectory endpoint frequency distributions indicating locations of possible entrainment points of microplastic for samples collected **a** before (samples 1–3), **b** during (samples 4–6), and **c** after (samples 7–11) the passage of Hurricane Larry over Newfoundland. To represent possible MP entrainment locations, only endpoints with elevation <1000 m were counted in the frequency summation.

points for pre-hurricane samples were mostly over the ocean, with only a few and low frequency trajectories crossing parts of Nova Scotia and Prince Edward Island (Fig. 5). Air parcels arriving during the hurricane have potential entrainment points over or close to the North Atlantic garbage patch (see location in Fig. 1) within the 48-h backwards time step, with the sample 6 model showing entrainment points through the middle of the garbage patch (Fig. 5).

Statistical analysis shows there is no significant correlation between the distance to the closest possible entrainment point and MP abundance ($r = 0.53$, $p = 0.11$; Supplementary Fig. 10). Also, no significant correlation exists between the size distribution of MP particles found in the samples and the distance from possible entrainment points and between the average distance the air masses travelled and the dominant polymer type in a sample. In pre-hurricane samples, the possible entrainment points are tightly packed together and are mostly within a 500 km radius. Conversely, possible entrainment points during and after the hurricane are spread over a much larger area, with some entrainment points >3000 km away from the sampling location (Fig. 5). Possible entrainment points have the greatest range in distance for sample 6, which also had the highest numbers of total particle and MP deposition. Air parcel trajectories for post-hurricane samples were all relatively similar, with on average higher frequencies per grid square, while trajectories for samples collected during the hurricane have a greater spread and are more variable (Fig. 5). For this model, estimated total error ranges between 15 and 30% of the travel distance[50] and is largely due to inaccuracies in the meteorological fields (wind speed and direction) used to drive the HYSPLIT model. However, the calculated back-trajectories only represent the centerline of a dispersing plume of emitted material, and so, a trajectory does not have to pass directly over an entrainment point for emissions from that point to have impacted the sample. A sensitivity analysis was also performed by starting the model from different elevations, showing there was relatively little variation by changing this parameter (Supplementary Fig. 9).

Source of MP. Hurricane Larry followed a northward trajectory over the northwest Atlantic Ocean, with the eye of the hurricane staying several hundred kilometres offshore of the east coast of North America until making landfall (Fig. 1). This implies that the hurricane did not pass over any highly polluted urban terrestrial areas, which are considered a source of airborne MPs[51], before hitting the sample site, which is also far from urban areas.

Hurricane Larry did pass over the North Atlantic garbage patch in the Sargasso Sea[37], where concentrations of up to 580,000 MP particles/km[2] in surface waters have been estimated previously[37]. Additionally, Hurricane Larry passed over the Labrador Current, which brings waters from the Arctic Ocean[52], where studies have found concentrations up to 282 MPs (>50 μm) m[−3] in sub-surface (7 m depth) waters[53]. Considering the abundance of MPs in surface waters in Hurricane Larry's path (and associated regions of extreme meteorological conditions) and the back-trajectory calculations, it is highly likely that the high amounts of MPs found in all the samples were sourced predominantly from those marine environments (Fig. 4). Although calculations are uncertain, previous studies have estimated that the ocean is the most dominant source for the atmospheric limb of the global MP cycle[49,54].

In samples 2–11, the most dominant polymer type is PMMA, which accounts for a maximum of 26% of the total MPs. This polymer type is often used in marine industrial activities because of its resistance to biofouling from algae or marine bacteria[55]. Nylon/PA is commonly used in fishing gear such as nets[56], providing further evidence in addition to the back-trajectory models that the MPs found in the samples were likely sourced from the ocean. PLS is a highly resistant thermoplastic used as a substitute for glass or metal by some industries[57], such as offshore petroleum production, which is present in the region affected by Hurricane Larry. The abundance of PLS in these samples can be linked to such activities. A major source of acrylic and PES MPs is synthetic fibres from clothing, with abundances of these polymers generally high in wastewater effluent[16], meaning these particles were likely sourced on land and transported to the ocean before being resuspended into the atmosphere. The diversity of polymer types in these samples shows that the MPs did not come from one source. Even though the back-trajectory calculations show that the particles may have been entrained over a large area, there is not much change in the proportions of each polymer type across these samples, likely indicating that MPs in the samples were picked up from the ocean where there is a relatively even distribution of polymers[58], as most MP in the marine environment are sourced on land and are transported throughout the ocean indiscriminately[59,60].

Strong hurricane winds have the potential to increase quantities of MPs picked up from the ocean by amplifying bubble injection and wave exchange processes[21]. The MPs entrained in the hurricane are then able to be transported far distances through the atmosphere, and as the hurricane weakens

over land or colder waters, the MP suspended by the storm are deposited. There is also potential for hurricanes to alter the normal trajectory of MP through the atmosphere and transport them further than in fair-weather conditions. Our back-trajectory model indicates that there were potential entrainment points of MP within a 100 km radius (Fig. 5), with the closest potential entrainment point (sample 1) located approximately 20 km away from the sampling location (Supplementary Table 1). However, the air masses did not pass over areas that could be considered a source of MPs. This study is the first demonstration of a hurricane as a mechanism for large-scale transport and deposition of MPs to a remote area.

Potential effects of atmospheric plastic pollution. The recognition that hurricanes may have the potential to disperse and deposit large amounts of MPs is concerning as there are several effects on the local environment. The toxic chemicals added to polymers, such as endocrine-disrupting phthalates, can leech directly into ecosystems[61], affecting the organisms living there. Additionally, MPs can act as transport vectors for contaminants such as heavy metals and viruses, carrying them between ecosystems or into humans[62]. Studies have found that ingestion of MPs by biota such as zooplankton in aquatic ecosystems, both marine and freshwater, can lead to significantly decreased algal feeding and therefore decreased function and health of the organism[5]. This may have adverse effects on higher trophic levels[63,64], though there is a current lack of data on the bioaccumulation of MPs. Newfoundland has many lakes with limited riverine input or output, and thus MPs deposited in these lakes are likely to stay for a long time, affecting micro- and potentially macro-organisms[65,66]. Potential ingestion of MPs by microorganisms in soils and other terrestrial environments poses the same threat as to those in aquatic environments, though there is currently significantly less research conducted on terrestrial biota than marine. MPs in both aquatic and terrestrial environments could negatively impact biodiversity in relatively undisturbed ecosystems not only across Newfoundland, but also in other locations that experience major storms. Increasing deposition of MPs in rural areas may also affect the humans living there as drinking water, sourced from wells fed by groundwater, may become contaminated with MPs. The sizes of MPs found in this study were small enough to be transported through pores of sandy or silty sediment, meaning they are able to be transported by groundwater[67], and may enter aquifers through deposition into and subsequent leaching from lakes or soils. Due to their small size and because they are already airborne, atmospheric MPs can enter organisms, including humans, also through respiration, the health consequences of which are still largely unknown. Consequently, large-scale deposition of MPs from hurricanes may have severe consequences as it increases the exposure to atmospheric plastic pollution also in remote locations with otherwise good air quality.

While there are many concerns about MP for individual organisms and ecosystems, there is also the potential for large-scale effects of atmospheric MPs on climate. Airborne MPs have the ability to affect radiative forcing, meaning they are able to absorb and scatter radiation in the atmosphere[9]. The effect of this forcing may impact global warming or the natural structure and transfer of heat through the atmosphere. MPs also have the potential to adjust cloud formation and therefore affect rainfall patterns[68,69]. Being able to quantify the concentration of MPs in the atmosphere will also improve climate models determining the effects of atmospheric MPs, especially during events in which there is an elevated number of airborne MPs, such as Hurricane Larry.

Limitations and future work. This study was done as a preliminary pilot study aimed at quantifying MPs deposition from a hurricane event. Due to the nature of a hurricane allowing only limited warning of its occurrence and preparedness for the exact flow path of the event before it occurs, we were only able to set up one sampling vessel in one location. Ideally, we'd recommend deploying at least three sampling vessels and investigating at least three locations simultaneously in order to improve the robustness of data for rigorously assessing potential sample contamination using statistical methods and to determine spatial distribution patterns in polymer types and deposition amounts throughout a hurricane event. Unfortunately, we did not have the equipment to measure rainfall at the sample site, so we had to rely on data collected at Cape Race weather station, located approximately 60 km from the sample site. In future studies, we would ideally be able to measure precipitation, wind speed, and wind direction at the sample site. Furthermore, to fully quantify the full potential extent of the impact of future hurricanes on the deposition of MPs, we recommend the continued monitoring of multiple hurricane events, forming at different latitudes with different trajectories and strengths.

The HYSPLIT model—and particularly the meteorological model outputs that are used to drive the HYSPLIT model—used in this study have limitations in reconstructing the complex atmospheric dynamics during a hurricane. This includes the use of air parcel (trajectory) modelling instead of particle modelling due to the overall small size of the particles and since MPs are thought to behave differently to the non-plastic particles for which these models were originally designed. MPs have a larger variety of shapes and are often less spherical and have a much lower mass than non-plastic particles, affecting drag and settling velocity. Since Hurricane Larry was short and intense, a 48-h-long back-trajectory model was used to capture the event, however, it is recognised that a 48-h window might not allow us to reconstruct all of the most distal source locations for some of the samples. Future studies may sample for a longer period pre- and post-hurricane allowing a longer back-trajectory to develop a more complete picture of MP source locations and how they differ between hurricane and fair-weather conditions. Furthermore, future studies may include forward atmospheric fate and transport modelling from entrainment locations—that can be carried out with HYSPLIT and related models—recognising the uncertainties in deposition processes noted above.

Methods

Sample collection. MP samples were collected in a sterilised 1 m tall glass deposition collector vessel with a 200 mm diameter that was placed on the ground and firmly secured to 3 wooden stakes using black zip ties[1]. Black MPs are difficult to analyse using µRaman spectroscopy and Nile Red fluorescence and were discounted from sample findings to ensure minimised field contamination of the samples. The vessel was situated at the centre of a clearing, approximately 100 metres from the coast. The clearing presented an area with a higher elevation than the surrounding area, unobstructed by trees, houses, or other structures. Bulk deposition samples were collected every 6 h commencing September 9 and ending September 12, resulting in a total of 11 samples. The 6 hourly sample duration was selected due to the hazardous nature of collecting deposition samples during the hurricane, acknowledging that hourly samples would have been preferable. The site was selected due to its accessibility, proximity to the coast, and remoteness. It was relatively remote and surrounded on 3 sides by ocean, ensuring there were no direct local point sources of MPs.

At the beginning of each sampling period, the sampling vessel was filled with 100 mL Milli-Q water, and the relative wind speed

and approximate direction were recorded. Since an anemometer was not available, wind speed was recorded using the Beaufort scale, and wind direction was based on visual cues. After 6 h, the contents of the vessel were decanted into a sterilised glass jar. The sides of the deposition collector vessel were rinsed three times with an additional 100 mL Milli-Q into the jar[41]. The jar was then firmly shut, labelled, and wrapped in aluminium foil ready for transport back to the laboratory. Field blanks ($n = 3$) were created following sample protocol for the first, middle, and last samples to account for contamination during sample collection. Precise separation between wet and dry deposition was not possible during the hurricane due to safety concerns so samples were labelled as bulk deposition.

Sample contamination was minimised by taking extra precautions both during sample collection and sample analysis. The sample collection vessel was always approached from downwind and rinsed three times with Milli-Q at the end of each sampling period into the jar with the sample. The jars were wrapped in aluminium foil and paper and stored upright in a cardboard box. They were also transported upright and stored in a 4 °C fridge in these boxes until laboratory analysis could begin. Field blanks were created as full process control blanks that went through all the same steps as the samples. Blanks were also created during laboratory MPs extraction, plus positive controls of spiked samples, to account for potential contamination and sample loss during processing. Glassware was used during both sample collection and analysis. Glassware was rinsed three times with Milli-Q and covered with aluminium foil after every use and between samples.

Laboratory sample preparation and analysis. Samples were transported to a dedicated MP analysis laboratory where they were digested to remove organic material, density separated for sediment and mineral particulate removal and then filtered onto aluminium oxide filters. Surfaces were cleaned with a paper towel and Milli-Q then covered in aluminium foil every week, while the entire laboratory underwent a thorough cleaning with Milli-Q each week. During digestion, sample temperatures were consistently checked to ensure the samples remained under 50 °C so as to not damage any plastic particles. The volume of each sample was recorded prior to any sample preparation activities and samples were analysed in triplicate. Samples were filtered onto 1.2 μm Whatman glass fibre filters (GF/C, 47 mm diameter) and the filtered residual material was digested using 30% w/w hydrogen peroxide (H_2O_2) in sterilised, covered borosilicate glass test tubes at 50 °C (dry block) for 48 h. Samples were then vacuum filtered (1.2 μm pore GF/C 47 mm diameter filters) and the remaining material was placed into density separation flasks with 1.6 g cm^{-3} zinc chloride solution ($ZnCl_2$) for a further 48 h. The suspended particles in $ZnCl_2$ (upper ½ of the density separation flask) were then filtered onto 25 mm diameter aluminium oxide filters in preparation for μRaman analysis. All filters were stored individually in 50 mm diameter sterilised aluminium containers to minimise sample contamination.

All samples were analysed using μRaman spectroscopy followed by Nile Red fluorescence microscopy. MP particle counts and polymer composition results are derived directly from μRaman analysis (Supplementary Data 1), with fluorescence microscopy providing the particle size distribution results (Supplementary Data 2). μRaman analysis was undertaken using a Renshaw InVia spectrometer with a 780 nm wavelength laser, 1200 gr mm-1 grating, and using up to 25% power (filter). Spectra were collected over 200–3000 cm^{-1} using a minimum of 5 acquisitions of 10 s. Filters were analysed using the sub-sampling method presented in Huppertsberg and Knepper[70] to ensure a representative 25% of each filter was analysed ($n = 2873$ particles). μRaman spectra for each particle were then individually analysed using Spectragryth, the SLOPP, SLOPPE, Simple[71–73] and inhouse reference libraries to identify if each particle was plastic and the respective polymer type. Only spectra with an 80% or greater accuracy were considered and counted as plastic polymers to ensure a conservative approach to the analysis was undertaken. Each filter was analysed three times to calculate an average count and an error of one standard deviation (1σ). The Limit of Quantification (LoQ) for this analysis (and the subsequent fluorescent analysis) was set to 1.2 μm, acknowledging that the limit of detection for μRaman is lower than this (1 μm).

After completion of μRaman analysis, all samples underwent fluorescent microscopy for particle size distribution assessment (necessary due to the limited clarity of μRaman visuals and the absence of particle finder software within the μRaman setup). Filters were dyed using 0.1 μg mL^{-1} Nile Red solution (powder dissolved in 99% pure ethanol (Sigma Aldrich), prefiltered through 1.2 μm GF/C filter), air dried overnight in a 30 °C oven (covered in sterilised foil to minimise sample contamination), and then placed in a dark, 4 °C fridge prior to analysis. Fluorescence microscopy was completed using an OMAX microscope and imaged using the AmScope MU500 camera and software, with 5% of the sample assessed and the images analysed using FIJI (ImageJ)[74]. Particles were classified as fragments or fibres, with fibres defined as particles with at least a 3:1 length-to-width ratio[44].

Back-trajectory modelling. Back-trajectory modelling was carried out with the HYbrid Single-Particle Lagrangian Integrated Trajectory (HYSPLIT) model version 5.2 using Global Data Assimilation System GDAS 1-degree archived global meteorology data (https://www.ready.noaa.gov/gdas1.php). Models were run for 48 h in backward mode from a starting elevation of half the planetary boundary layer (~500 m above mean sea level) calculated dynamically by the model at any given starting time above the sampler. The mid-boundary-layer starting height was chosen as it best represents the source of air in the well-mixed planetary boundary layer above the sampler. As a sensitivity test we ran back-trajectory simulations from a starting elevation of one-quarter and three-quarters of the planetary boundary layer and the results were not significantly influenced (see Supplementary Fig. 9). The hourly endpoints from each trajectory were summed over a 1-degree grid, and the gridded frequencies were calculated as the number of endpoints in a given grid square divided by the total number of endpoints in all of the trajectories being considered (see Supplementary Note 4). A new trajectory simulation was run for every hour within the sampling period, resulting in 66 individual trajectories, which were then mapped using Esri (ArcMap 10.4). We judged that any air parcels within 1000 m of the surface as possible entrainment points, as this lower section of the atmosphere experiences sufficient vertical mixing to transport MPs from the surface throughout this section of the air column relatively quickly[48].

Blanks, positive controls, and contamination mitigation. The field blanks were managed and assessed as full process blanks, representing not only the potential field contamination but also any sample contamination due to laboratory sample preparation and analysis. Spiked samples were also prepared and processed as positive controls to quantify analysis efficiency and accuracy. Sample blank and spike corrections were applied to MP counts from both Raman spectroscopy and Nile Red fluorescence analyses. Sample analysis was carried out in a clean laboratory outfitted with HEPA filters and restricted access, with all persons in

the laboratory required to wear 100% cotton clothing and laboratory coats. All processing steps were done under a laminar flow fume hood using glassware, while all liquids used, including chemicals and Nile red, were prefiltered using a filter of the same porosity used in sample filtration (1.2 μm GF/C filter).

Data availability

References

1. Allen, S. et al. Atmospheric transport and deposition of microplastics in a remote mountain catchment. *Nat. Geosci.* **12**, 339–344 (2019).
2. Bergmann, M. et al. White and wonderful? Microplastics prevail in snow from the Alps to the Arctic. *Sci. Adv.* **5**, 1–11 (2019).
3. Liu, K. et al. Consistent transport of terrestrial microplastics to the ocean through atmosphere. *Environ. Sci. Technol.* **53**, 10612–10619 (2019).
4. Zhang, Y., Gao, T., Kang, S. & Sillanpää, M. Importance of atmospheric transport for microplastics deposited in remote areas. *Environ. Pollut.* **254**, 1–4 (2019).
5. Cole, M. et al. Microplastic ingestion by Zooplankton. *Environ. Sci. Technol.* **47**, 6646–6655 (2013).
6. Schirinzi, G. F. et al. Cytotoxic effects of commonly used nanomaterials and microplastics on cerebral and epithelial human cells. *Environ. Res.* **159**, 579–587 (2017).
7. Karbalaei, S. et al. Abundance and characteristics of microplastics in commercial marine fish from Malaysia. *Mar. Pollut. Bull.* **148**, 5–15 (2019).
8. Marn, N., Jusup, M., Kooijman, S. A. L. M. & Klanjscek, T. Quantifying impacts of plastic debris on marine wildlife identifies ecological breakpoints. *Ecol. Lett.* **23**, 1479–1487 (2020).
9. Revell, L. E., Kuma, P., Le Ru, E. C., Somerville, W. R. C. & Gaw, S. Direct radiative effects of airborne microplastics. *Nature.* **598**, 462–467 (2021).
10. Walker, T. R., Wang, L., Horton, A. & Xu, E. G. Micro(nano)plastic toxicity and health effects: Special issue guest editorial. *Environ. Int.* **170**, 107626 (2022).
11. Drummond, J. D. et al. Microplastic accumulation in riverbed sediment via hyporheic exchange from headwaters to mainstems. *Sci. Adv.* **8**, eabi9305 (2022).
12. Li, W. C., Tse, H. F. & Fok, L. Plastic waste in the marine environment: a review of sources, occurrence and effects. *Sci. Total Environ.* **566-567**, 333–349 (2016).
13. Siegfried, M., Koelmans, A. A., Besseling, E. & Kroeze, C. Export of microplastics from land to sea. A modelling approach. *Wat. Res.* **127**, 249–257 (2017).
14. Allen, S., Allen, D., Karbalaei, S., Maselli, V. & Walker, T. R. Micro(nano) plastics sources, fate, and effects: what we know after ten years of research. *J. Hazard. Mater. Adv.* **6**, 100057 (2022a).
15. Andrady, A. L. Microplastics in the marine environment. *Mar. Pollut. Bull.* **62**, 1596–1605 (2011).
16. Browne, M. A. et al. Accumulation of microplastic on shorelines worldwide: Sources and sinks. *Environ. Sci. Technol.* **45**, 9175–9179 (2011).
17. Cole, M., Lindeque, P., Halsband, C. & Galloway, T. S. Microplastics as contaminants in the marine environment: a review. *Mar. Pollut. Bull.* **62**, 2588–2597 (2011).
18. Dubaish, F. & Liebezeit, G. Suspended microplastics and black carbon particles in the jade system, Southern North Sea. *Wat. Air Soil Pollut.* **224**, 1352 (2013).
19. Nyberg, B., Harris, P. T., Kane, I. & Maes, T. Leaving a plastic legacy: current and future scenarios for mismanaged plastic waste in rivers. *Sci. Total Environ.* **869**, 161821 (2023).
20. Brahney, J., Hallerud, M., Heim, E., Hahnenberger, M. & Sukumaran, S. Plastic rain in protected areas of the United States. *Science.* **368**, 1257–1260 (2020).
21. Allen, S. et al. Examination of the ocean as a source for atmospheric microplastics. *PLoS ONE* **15**, e0232746 (2020). 1 14.
22. Abbasi, S., Rezaei, M., Ahmadi, F. & Turner, A. Atmospheric transport of microplastics during a dust storm. *Chemosphere.* **292**, 133456 (2022).
23. Li, C. et al. Enhanced impacts evaluation of Typhoon Sinlaku (2020) on atmospheric microplastics in South China Sea during the East Asian Summer Monsoon. *Sci. Total Environ.* **806**, 150767 (2022).
24. NOAA Atlantic Oceanographic & Meteorological Laboratory. *Hurricanes Frequently Asked Questions.* (NOAA Atlantic Oceanographic & Meteorological Laboratory, 2021; https://www.aoml.noaa.gov/hrd-faq/).
25. Harriss, R. et al. Atmospheric transport of pollutants from North America to the North Atlantic Ocean. *Nature.* **308**, 722–724 (1984).
26. Steinnes, E. & Friedland, A. J. Metal contamination of natural surface soils from long-range atmospheric transport: Existing and missing knowledge. *Environ. Rev.* **186**, 169–186 (2006).
27. O'Dowd, C. D. & de Leeuw, G. Marine aerosol production: a review of the current knowledge. *Philos. Trans. R. Soc. London, Ser. A.* **365**, 1753–1774 (2007).
28. Quinn, J. A., Steinbrook, R. A. & Anderson, J. L. Breaking bubbles and the water-to-air transport of particulate matter. *Chem. Eng. Sci.* **30**, 1177–1184 (1975).
29. Pan, Y. et al. Wet deposition and scavenging ratio of air pollutants during an extreme rainstorm in the North China Plain. *Atmos. Oceanic Sci. Lett.* **10**, 348–353 (2017).
30. Sassen, K. et al. Midlatitude cirrus clouds derived from hurricane Nora: A case study with implications for ice crystal nucleation and shape. *J. Atmos. Sci.* **60**, 873–891 (2003).
31. Bhandari, S. et al. Spatial and temporal analysis of impacts of hurricane florence on criteria air pollutants and air toxics in eastern North Carolina. *Int. J. Environ. Res. Public Health.* **19**, 1757 (2022).
32. Brown, D. P. National Hurricane Centre tropical cyclone report: hurricane Larry. *Tech. Rep. AL122021* (National Hurricane Centre, 2021).
33. Statistics Canada. *Focus on Geography Series, 2011 Census (Stats. Can. Cat. No. 98-310-XWE2011004, 2012;* https://www12.statcan.gc.ca/census-recensement/2011/as-sa/fogs-spg/Facts-pr-eng.cfm?Lang=eng&GC=35).
34. Government of Newfoundland and Labrador. *Industry, Energy and Technology* (Government of Newfoundland and Labrador, 2023; https://www.gov.nl.ca/iet/).
35. Darack, E. Avalon Peninsula, Canada. *Weatherwise* **59**, 14–15 (2006).
36. Plante, M., Son, S., Atallah, E. & Grise, K. Extratropical cyclone climatology across eastern Canada. *Int. J. Climatol.* **35**, 2759–2776 (2015).
37. Law, K. L. et al. Plastic accumulation in the North Atlantic subtropical gyre. *Science* **329**, 1185–1188 (2010).
38. Abbassi, S. Microplastics washout from the atmosphere during a monsoon rain event. *J. Hazard. Mater* **4**, 1000035 (2021).
39. Hamilton, B. M. et al. Microplastics around an Arctic seabird colony: Particle community composition varies across environmental matrices. *Sci. Total Environ.* **773**, 145536 (2021).
40. Cai, L. et al. Characteristic of microplastics in the atmospheric fallout from Dongguan city, China: preliminary research and first evidence. *Environ. Sci. Pollut. Res.* **24**, 24928–24935 (2017).
41. Dris, R., Gasperi, J., Saad, M., Mirande, C. & Tassin, B. Synthetic fibers in atmospheric fallout: a source of microplastics in the environment? *Mar. Pollut. Bull.* **104**, 290–293 (2016).
42. Knutson, T. R. et al. In *Critical Issues in Climate Change Science* (eds C. Le Quéré, C. et al.) Ch. 5 (ScienceBrief, 2021).
43. Hidalgo-Ruz, V., Gutow, L., Thompson, R. C. & Thiel, M. Microplastics in the marine environment: a review of the methods used for identification and quantification. *Environ. Sci. Technol.* **46**, 3060–3075 (2012).
44. Löder, M. & Gerdts, G. In *Marine Anthropogenic Litter* (Bergmann, M. et al.) Ch. 5 (Springer, 2015).
45. Goossens, D. Wind tunnel calibration of the USGS dust deposition sampler: Sampling efficiency and grain size correction. *Aeolian Res* **2**, 159–170 (2010).
46. Stein, A. F. et al. NOAA's HYSPLIT atmospheric transport and dispersion modeling system. *Bull. Amer. Meteor. Soc.* **96**, 2059–2077 (2015).
47. Rolph, G., Stein, A. & Stunder, B. Environmental modelling & software Real-time Environmental Applications and Display sYstem: READY. *Environ. Modell. Software* **95**, 210–228 (2017).
48. Angevine, W. M., White, A. B. & Avery, S. K. Boundary-layer depth and entrainment zone characterization with a boundary-layer profiler. *Boundary-Layer Meteorol* **68**, 375–385 (1994).
49. Evangeliou, N., Tichý, O., Eckhardt, S., Zwaaftink, C. G. & Brahney, J. Sources and fate of atmospheric microplastics revealed from inverse dispersion modelling: from global emissions to deposition. *J. Hazard. Mater.* **432**, 128585 (2022).
50. Draxler, R. R., Rolph, G. D. & Stunder, B. J. B. *HYSPLIT PC Training Seminar.* (National Oceanic and Atmospheric Administration Air Resources Library, 2007) https://www.arl.noaa.gov/documents/workshop/Spring2007/HTML_Docs/index.html.
51. Wright, S. L., Ulke, J., Font, A., Chan, K. L. A. & Kelly, F. J. Atmospheric microplastic deposition in an urban environment and an evaluation of transport. *Environ. Int.* **136**, 105411 (2020).

52. Loder, J. W., Petrie, B. & Gawarkiewicz, G. In *The Sea* (eds Robinson, A. R. & K. H. Brink, K. H.) Vol. 11, Chap. 5 (Wiley, 1998).
53. Jones-Williams, K., Galloway, T. S., Peck, V. L. & Manno, C. Remote, but not isolated—microplastics in the sub-surface waters of the Canadian Arctic Archipelago. *Front. Mar. Sci.* **8**, 1–13 (2021).
54. Brahney, J., Mahowald, N., Prank, M. & Prather, K. A. Constraining the atmospheric limb of the plastic cycle. *Proc. Natl Acad. Sci. USA* **118**, e2020719188 (2021).
55. Dibke, C., Fischer, M. & Scholz-Böttcher, B. M. Microplastic mass concentrations and distribution in German bight waters by pyrolysis—gas chromatography—mass spectrometry/ thermochemolysis reveal potential impact of marine coatings: do ships leave skid marks? *Environ. Sci. Technol.* **55**, 2285–2295 (2021).
56. Thomas, S. N. & Hridayanathan, C. The effect of natural sunlight on the strength of polyamide 6 multifilament and monofilament fishing net materials. *Fish. Res.* **81**, 326–330 (2006).
57. Yu, L., Zhao, D. & Wang, W. Mechanical properties and long-term durability of recycled polysulfone plastic. *Waste Manage* **84**, 402–412 (2019).
58. Erni-Cassola, G., Zadjelovic, V., Gibson, M. I. & Christie-Oleza, J. A. Distribution of plastic polymer types in the marine environment; a meta-analysis. *J. Hazard. Mater.* **369**, 691–698 (2019).
59. Geyer, R., Jambeck, J. R. & Law, K. L. Production, use, and fate of all plastics ever made. *Sci. Adv.* **3**, 3–8 (2017).
60. Jambeck, J. R. et al. Plastic waste inputs from land into the ocean. *Science* **347**, 764–768 (2015).
61. Dusaucy, J., Gateuille, D., Perrette, Y. & Naffrechoux, E. Microplastic pollution of worldwide lakes. *Environ. Pollut.* **284**, 117075 (2021).
62. Wang, J. et al. Typhoons increase the abundance of microplastics in the marine environment and cultured organisms: a case study in Sanggou Bay, China. *Sci. Total Environ.* **667**, 1–8 (2019).
63. Eriksson, C. & Burton, H. Origins and biological accumulation of small plastic particles in fur seals from Macquarie island. *AMBIO: J. Hum. Environ.* **32**, 380–384 (2003).
64. Romeo, T. et al. First evidence of presence of plastic debris in stomach of large pelagic fish in the Mediterranean Sea. *Mar. Pollut. Bull.* **95**, 358–361 (2015).
65. Lusher, A., Hollman, P. & Mendoza-Hill, J. *Microplastics in Fisheries and Aquaculture. Status of Knowledge on Their Occurrence and Implications for Aquatic Organisms and Food Safety.* (FAO Fisheries and Aquaculture Tech. Rep. 615, 2017).
66. Rochman, C. M. et al. Rethinking microplastics as a diverse contaminant suite. *Environ. Toxicol. Chem.* **38**, 703–711 (2019).
67. Viaroli, S., Lancia, M. & Re, V. Microplastics contamination of groundwater: current evidence and future perspectives. A review. *Sci. Total Environ.* **824**, 153851 (2022).
68. Allen, D. et al. Microplastics and nanoplastics in the marine-atmosphere environment. *Nat. Rev. Earth Environ.* **3**, 393–405 (2022b).
69. Aeschlimann, M., Li, G., Kanji, Z. A. & Mitrano, D. M. Potential impacts of atmospheric microplastics and nanoplastics on cloud formation processes. *Nat. Geosci.* **15**, 967–975 (2022).
70. Huppertsberg, S. & Knepper, T. P. Instrumental analysis of microplastics—benefits and challenges. *Anal. Bioanal. Chem.* **410**, 6343–6352 (2018).
71. Menges, F. *Spectragryph—Optical Spectroscopy Software, Version 1.2.14* (2020), http://www.effemm2.de/spectragryph/.
72. Munno, K., De Frond, H., O'Donnell, B. & Rochman, C. M. Increasing the accessibility for characterizing microplastics: introducing new application-based and spectral libraries of plastic particles (SLoPP and SLoPP-E). *Anal. Chem.* **92**, 2443–2451 (2020).
73. Primpke, S. et al. Toward the systematic identification of microplastics in the environment: evaluation of a new independent software tool (siMPle) for spectroscopic analysis. *Appl. Spectrosc.* **74**, 1127–1138 (2020).
74. Schindelin, J. et al. Fiji: an open-source platform for biological-image analysis. *Nat. Methods.* **9**, 676–682 (2012).
75. Eriksen, M. et al. Plastic pollution in the world's oceans: more than 5 trillion plastic pieces weighing over 250,000 tons afloat at sea. *PLoS ONE* **9**, 1–15 (2014).

Author contributions
A.C.R. conceived the study, collected and analysed field samples, performed the back-trajectory modelling, wrote the manuscript, and drafted the figures. D.A. analysed the samples, contributed to the back-trajectory modelling and drafting of the manuscript and figures. S.A. analysed the samples and contributed to the drafting of the manuscript. V.M. conceived the study, contributed to the drafting of the manuscript and figures. A.L.B. contributed to sample collection. L.K. supported data analysis. S.K. supported data analysis. T.R.W. contributed to the drafting of the manuscript. M.C. supported the back-trajectory modelling. A.C.R., V.M., T.R.W., and N.C. contributed to the final editing of the manuscript.

Competing interests
The authors declare no competing interests.

Additional information
Supplementary information The online version contains supplementary material available at https://doi.org/10.1038/s43247-023-01115-7.

Correspondence and requests for materials should be addressed to Anna C. Ryan or Vittorio Maselli.

Peer review information *Communications Earth & Environment* thanks Yanxu Zhang, Janice Brahney, and the other, anonymous, reviewer(s) for their contribution to the peer review of this work. Primary handling editors: Weiqing Han, Heike Langenberg. A peer review file is available.

Reprints and permission information is available at http://www.nature.com/reprints

Publisher's note Springer Nature remains neutral with regard to jurisdictional claims in published maps and institutional affiliations.